10.7

THE ITWS RUNWAY WIND NOWCAST PRODUCT

R. Gary Rasmussen and Frank M. Robasky

MIT Lincoln Laboratory
244 Wood Street
Lexington, Massachusetts 02173-9108

1. INTRODUCTION

The Runway Wind Nowcast Product[1] will support the ITWS[2] objective by providing short term (up to 30 minutes) forecasts of the tailwind and crosswind components of the horizontal wind over each runway at an ITWS airport. These forecasts will enable FAA users to better anticipate wind shifts impacting runway usage and trajectories of approaching and departing air traffic. They may also support future ITWS products such ceiling and visibility nowcasts.

Our initial development efforts, which are reported here, have been directed toward Orlando International Airport (MCO) as the product request originated there. However, in the near future we plan to expand the scope to include other ITWS airports including Memphis.

The Runway Wind Nowcast Product is being developed to help Air Traffic Control (ATC) personnel answer the following question: Do we need to change runways? That would become necessary if tailwinds or crosswinds exceed usage thresholds. At most US airports, with dry runways, tailwinds must be less than five knots and crosswinds must be less than 15 knots. Other, lower thresholds apply if the runways are wet. However, these thresholds are subject to local modifications. For example, the MCO tailwind threshold for dry runways is 7 knots.

The decision faced by ATC personnel seems, at first, to be clear cut: if the tailwind or crosswind exceeds nominal thresholds, use of that runway must be discontinued. The problem (at least at MCO) is that most threshold crossings are very brief. So, it may be better to temporarily hold traffic than to switch runways. Reliable (*i.e.*, accurate and precise) short term forecasts will help ATC personnel make better hold-or-switch decisions.

2. BACKGROUND INFORMATION

2.1 *Event Statistics*

How frequently are hold-or-switch decisions required? To gain insight into this question we compiled statistics on the frequency and duration of runway usage threshold-crossing events using 111 days of Low Level Windshear Alert System (LLWAS) wind observations taken at MCO. In the future, we also plan to analyze runway usage logs.

The LLWAS data set was collected in 1992 between June and September. This is the rainy season in Orlando and most of the observed events were due to local flows associated with convective storms. The MCO LLWAS system consists of a network of 14 anemometers arranged in three lines, each orientated north-south. The three MCO runways have a like orientation (Fig. 1). In Orlando, the preferred flow for

---

1 The work described here was sponsored by the Federal Aviation Administration (FAA). The United States Government assumes no liability for its content or use thereof.

2 The Integrated Terminal Weather System (ITWS) currently in development by the FAA will be a fully automated, integrated terminal weather information system designed to improve the safety, efficiency, and capacity of terminal area aviation operations. The ITWS will acquire data from FAA and National Weather Service sensors as well as from aircraft in flight in the terminal areas of selected airports. It will provide products to FAA Air Traffic personnel that are immediately usable without further meteorological interpretation. Those products include current terminal area weather and short term predictions of significant weather phenomena.

arriving and departing air traffic is from north to south. In that runway configuration a north wind is a tailwind. Since we didn't know which configuration was in use at any given time, we compiled statistics for north wind events rather than for tailwind events. Figure 2 shows the results.

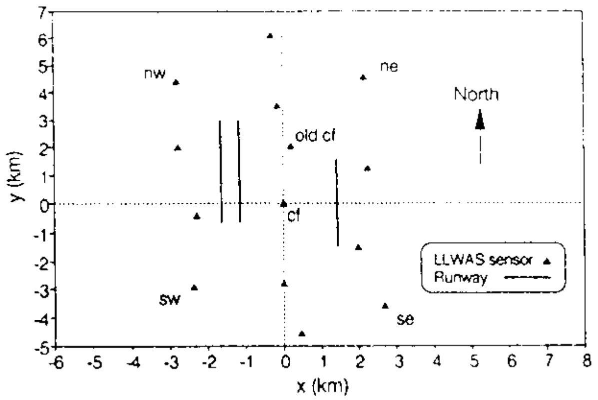

Figure 1. Schematic map of Orlando International Airport (MCO) showing runway and LLWAS sensor locations.

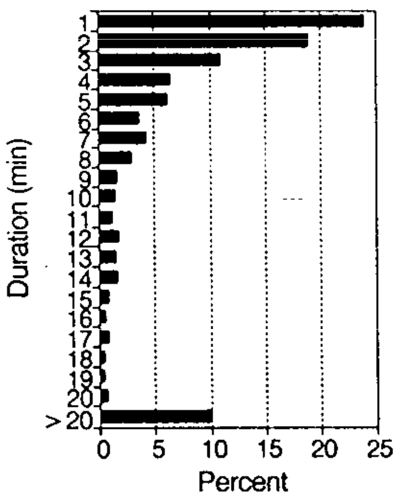

Figure 2. Relative frequency (N=747) of durations of north winds greater than 7 knots showing that long-duration threshold-crossing events are relatively uncommon.

During the 111 days of the study period 747 threshold-crossing north-wind events occurred: an average of 6.7 per day. Eighty percent had durations of 10 minutes or less (5.4 per day) while 10 percent (0.7 per day) had durations greater than 20 minutes. The median duration was three minutes. For crosswind, which has a higher threshold, threshold-crossing events were less common. 187 events occurred during the 111 days of which 91 percent had durations of 10 minutes or less. Five events (1 per 22 days) had durations greater than 20 minutes. Again, the median duration was three minutes.

As most threshold-crossing events are associated with convective storms, it is not surprising that their number peaks in the mid to late afternoon. During the study period nearly half of the north-wind events with durations of 10 minutes or less occurred between noon and 8 PM (local time). The peak occurred between 4 and 6 PM. That this time coincides with the afternoon traffic surge further emphasizes the need for reliable short-term wind forecasts.

2.2 *Data Sources*

The Runway Wind Nowcast Product will rely primarily on observations from a local network of LLWAS or Automated Surface Observing System (ASOS) anemometers. A simple scale analysis shows that a typical network radius of about 5 km will support a 15 minute forecast, assuming a disturbance propagation speed of 5 m/s. For higher propagation speeds and longer forecasts (30 minutes is desired) we must gather wind information from a larger area around the airport. Thus, we also plan to use Doppler radar wind observations, as processed by the ITWS Terminal Wind Analysis Product (Cole *et al.*, 1993) and the Machine Intelligent Gust Front Algorithm (Delanoy and Troxel, 1993). Figure 3 summarizes these relationships.

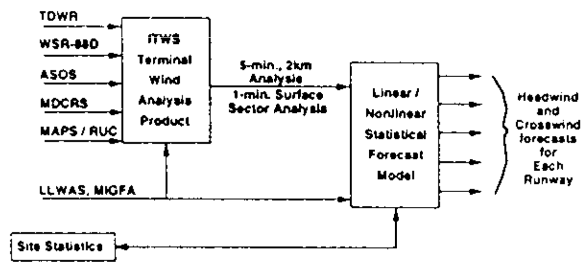

Figure 3. Schematic diagram showing the Runway Wind Nowcast Product inputs and outputs.

2.3 *User Interface*

Our preliminary concept for a user interface is to present two levels of information. Normally, the user display will show a color-coded status circle which, when activated, will expand to show a time series of crosswind and tailwind for the selected runway. The color code will be as follows:

- *red* — a threshold crossing is forecast to occur during the next 10 minutes,
- *yellow* — a crossing (the first) is forecast to occur from 10 to 30 minutes hence,
- *green* — no crossings are forecast over the next 30 minutes, and
- *black* — the forecast system is not currently operational (e.g., insufficient data).

The time series display will show the actual wind components over the past 30 minutes and future projections for up to 30 minutes. Estimates of forecast reliability will be made too, but will not be displayed. Rather, they will be used to suppress forecasts which are deemed to be insufficiently reliable (Fig. 4).

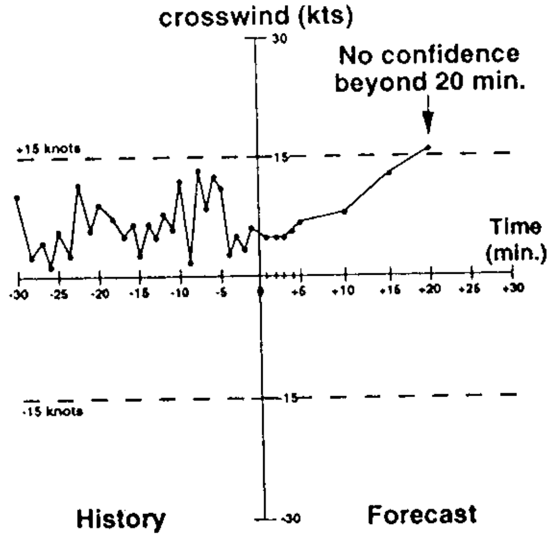

Figure 4. Tentative user display of crosswind series. In this example estimates of low forecast precision inhibit forecast displays for lead times greater than 20 minutes.

2.4 *Forecasting Approach*

Linear and non-linear time series (Gershenfeld and Weigend, 1993) and space-time models are being evaluated for use in a Kalman Filter (*i.e.*, state space) framework (Harvey, 1989; Gelb, 1974) to generate headwind and crosswind forecasts. Although we plan to employ as much physics as feasible, data limitations mandate use of a statistical approach.

We anticipate a need to customize forecast model parameters for each ITWS airport (as well as for diurnal and annual cycles). This presents an implementation dilemma in that an adequate development database is not expected to be available prior to the initial installation at some sites. To ameliorate this problem, we plan to integrate a learning algorithm and a local statistics database with the forecast model so that site performance will improve over time. Moreover, we will use proxy data during development where feasible.

3. PROGRESS

3.1 *Preliminary Data Processing*

LLWAS wind speeds and directions are sampled every 10 seconds. All results discussed below are based on simple two minute trailing averages of the u and v components of the observed winds. The running means have been resampled at one or five minute intervals.

As noted above, the MCO LLWAS network contains 14 sensors. Measurements from these sensors can be in marked disagreement, as is illustrated in Figure 5. These inconsistencies may be the result of true variations in the wind field, improperly sited sensors, obstructions, faulty instruments, or a combination of these factors. Traditionally, ATC personnel consult the center field anemometer when making decisions about runway usage. Ironically, the reported center field LLWAS speed at MCO may be biased high, compared with speeds from other network sensors. Another consideration is frequently missing data, with some sensors more prone to dropouts than others. These aspects of the LLWAS data imply that a real-time data quality module will be an essential component of an operational product generator.

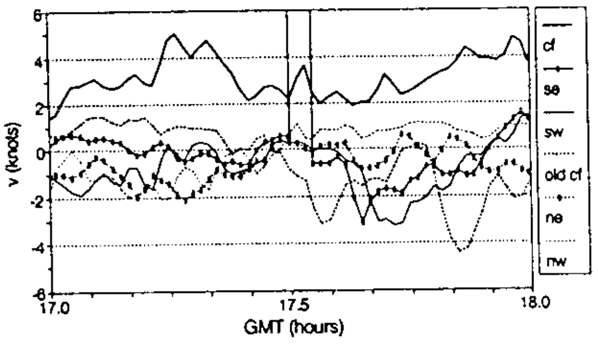

Figure 5. Measurements of the v wind component from 6 of the 14 MCO LLWAS sensors for a 1-hour period on 9/21/92, illustrating center field sensor bias. The vertical solid lines near 1730 GMT bound a data dropout in the southeast sensor.

After some experimentation, we decided to fit a linear (spatial) surface to the available LLWAS observations of each wind component at each time. The least-squares fit was of the form:

$$w(x,y) = c_0 + c_1 x + c_2 y \qquad (1)$$

where w is either u or v, x and y are rectangular coordinates of the sensors (with the origin at center field, see Fig. 1), and c_0, c_1, and c_2 are parameters of the fit. Note that c_0 is the fitted value at center field, c_1 is an estimate of $\partial w/\partial x$, and c_2 is an estimate of $\partial w/\partial y$. We fit a plane rather than a higher order polynomial surface to suppress higher spatial frequencies. The fitting also tended to beneficially suppress higher temporal frequencies and biases (Fig. 6).

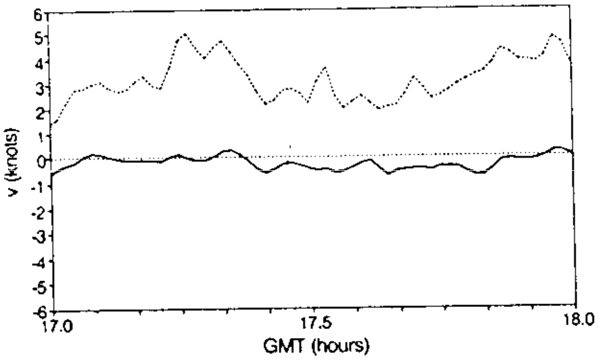

Figure 6. The observed center field v (dotted line) and its estimate from a linear surface fit to all available sensors (solid line) showing that the estimate filters high temporal frequencies and removes most of the center field measurement bias (compare with Fig. 5).

3.2 *Statistical Forecast Models*

Initial efforts have focused mainly on developing and applying a conventional linear time series model: the autoregressive, integrated, moving average (ARIMA) model of Box and Jenkins (1976). These results will serve as a baseline for the subsequent evaluation of nonlinear and space-time models. The general form of an ARIMA(p,d,q) model is:

$$\left(1 - \sum_{i=1}^{p} a_i B^i\right)(1-B)^d w_t = C + \left(1 - \sum_{j=1}^{q} b_j B^j\right)\varepsilon_t \qquad (2)$$

$$B^i w_t = w_{t-i}$$

Here, B is the backshift operator, C is a constant, and a_i and b_i are autoregressive (AR) and moving average (MA) coefficients, respectively. $\{\varepsilon_t\}$ is a series of random shocks (unobserved inputs) which are assumed to be both zero mean and independently and identically distributed. $\{w_t\}$ is the subject time series (which may be a transformed version of an original series). In the present case it is either $\{u_t\}$ or $\{v_t\}$. Note that Eq. 2 may be solved for w_t. This gives a one-step prediction formula. An n-step prediction may be obtained by iterating the 1-step formula. Thus, with this model, predictions of future winds are based purely on past behavior, an obvious weakness.

In practice, the ARIMA modeling process consists of several iterations of the following steps:

- identify p, d, and q, the autoregressive, difference, and moving average orders, using graphical or analytical tools (this is the most difficult step),
- estimate the coefficients using a maximum likelihood or least-squares procedure to minimize 1-step ahead forecast errors, and
- perform diagnostic checks to determine the adequacy of the model.

Initially, we developed low order models using several days of data. Model parameters were identified using an objective criterion which minimized 1-step prediction errors while penalizing models for large p's and q's. The resulting models perform well for 1 or 2 steps, but the prediction accuracy degrades rapidly at longer leads. For example, Fig. 7 shows several 30-minute forecasts from an ARIMA(2,1,1) model for u on 8/28/92 using a 5-minute time step. This case is interesting because of a dramatic rise and fall in the crosswind component of roughly 10 knots within a 1.5 hour time period, with the wind briefly crossing the usage threshold. The north-wind component, although not shown, is equally interesting as it drops quickly to just short of the tailwind threshold and then slowly rises.

In Fig. 7, short-lead forecasts are seen to be much more accurate than those at longer leads for the points of most interest: the turning points. It is apparent that we should optimize this model for longer leads (*i.e.*, more than 1 step ahead). Moreover, in cases such as this, a larger information set (*e.g.*, supplemental gradient information) should be beneficial. Figure 8 shows that, over the entire day, the ARIMA(2,1,1) model slightly outperforms persistence at all leads.

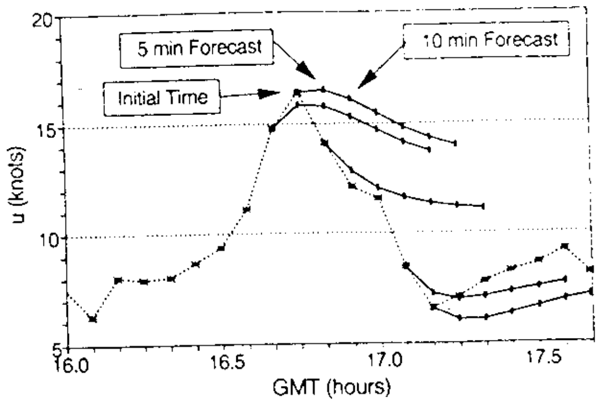

Figure 7. 5 to 30 minute forecasts from an ARIMA(2,1,1) model of u-wind for 8/28/92. Actual winds (asterisks) and forecasts (vertical ticks) have a sampling interval of 5 minutes.

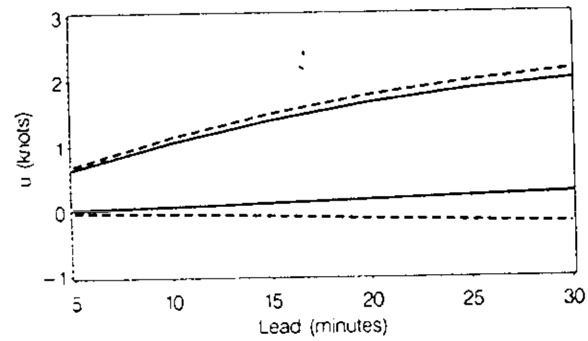

Figure 8. RMS error (upper curves) and bias (lower curves) as a function of forecast lead for 8/28/92 from the ARIMA(2,1,1) model of Fig. 7 (solid line) and persistence (dashed line).

What is the AR order beyond which no appreciable gain in forecast accuracy will be achieved? To investigate this question we fit AR models of varying order and observed the order at which, for selected forecast leads and independent data, the RMS forecast error is minimized. We used three days of 1-minute u data (8/27- 8/29) and applied the resulting models to this same period (dependent data) and also to an independent three day period (7/30-8/1). The results for 1-step forecasts are shown in Fig. 9. As expected, the model performs better with dependent data. The RMS forecast error with independent data is minimized at order 15 (though essentially at order 7). We obtained longer lead forecasts by iterating the 1-step model and found that for leads of 5 or more steps, the RMS error is minimized with a third or fourth order model. Thus it seems that little or no forecasting advantage at longer leads is gained from the use of higher order, iterated 1-step models. This confirms the need to develop forecast models optimized for longer lead (n-step) forecasts.

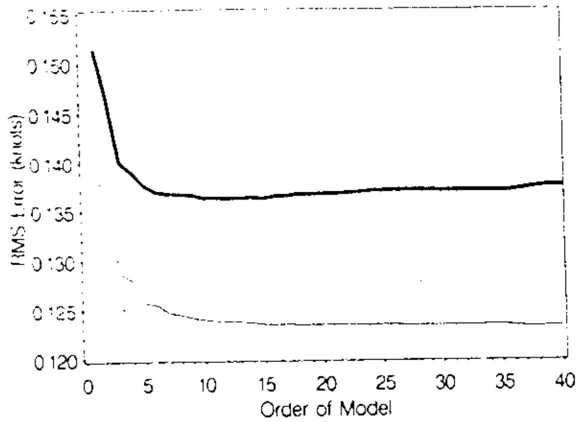

Figure 9. 1-step AR model RMS forecast error for 3-day dependent (lower line) and independent (upper line) data sets. The RMS error with independent data is minimized at order 15 but shows little improvement past order 7.

We mentioned earlier that spatial information should be helpful. Preliminary investigations in this direction were based on the spatial variations present within the MCO LLWAS network. Consider the Navier-Stokes equation for u (dx/dt):

$$\frac{\partial u}{\partial t} = -u\frac{\partial u}{\partial x} - v\frac{\partial u}{\partial y} - w\frac{\partial u}{\partial z} + fv - \frac{1}{\rho}\frac{\partial p}{\partial x} + F_x \qquad (3)$$

Here, x, y, and z are Cartesian coordinates, v is dy/dt, w is dz/dt, f is the Coriolis parameter, p is pressure, ρ is density, and F_x is the x component of the frictional force. Of the right hand side terms, only the first two (horizontal advection) and the fourth (Coriolis) can be calculated from the wind data at hand. However, for the spatial scales under consideration, the Coriolis force is small and will be ignored for the sake of this discussion.

We calculated the horizontal advection terms each minute using all LLWAS sensor data and Eq. 1. Figure 10 shows that the u-advection for the sample period of Fig. 7 has an advection maximum which precedes the maximum in u by about 5 minutes. Although not shown, the v-advection similarly anticipates changes in v. Thus advection may be a useful additional predictor.

We have begun to investigate another class of prediction models: feed-forward neural networks. The architecture of one model we have used is shown in Fig. 11. Observe that by connecting the input nodes (lowest layer) directly to the output, we could construct a corresponding (linear) AR model. The neural network's essential nonlinearity is due its activation function (a logistic function here). Although these networks have shown great promise by outperforming corresponding linear models, we have decided to postpone their further development until we settle on a linear model architecture as the corresponding linear models are much more economical to develop.

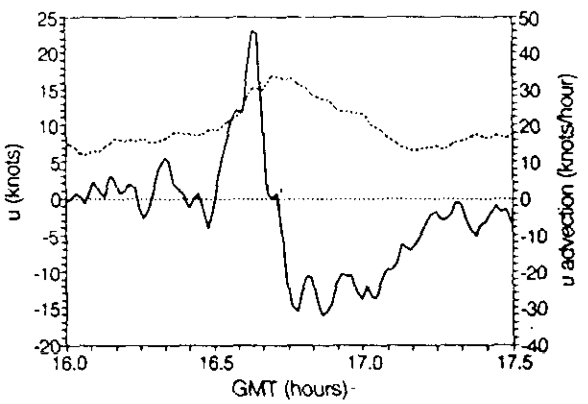

Figure 10. Horizontal u advection (solid line) and fitted center-field u (dotted line) on 8/28/92. Changes in advection are seen to precede changes in u.

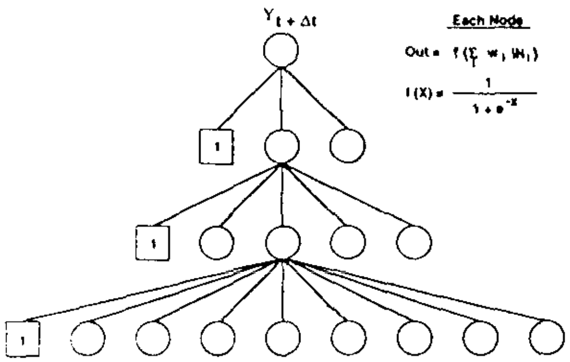

Figure 11. An example of a feed-forward neural network prediction architecture we have used. Lines between nodes (circles) represent weights. Only a small subset of weights in the fully connected architecture is displayed.

4. SUMMARY AND FUTURE PLANS

The Runway Wind Nowcast Product, now under development at Lincoln, will provide short-term (up to 30-minutes) forecasts of the crosswind and tailwind on each runway at ITWS airports. The forecast model will have both deterministic and stochastic components. Ultimately, the prediction algorithms will be embedded in a Kalman filter framework to permit dynamic updating of system parameters and to provide estimates of forecast precision. Initial work has focused on the use of univariate ARIMA models, which will provide a baseline against which to evaluate future models.

Our efforts will next be directed towards the development of longer lead models (*i.e.*, optimized beyond 1 step) and space-time models utilizing horizontal advection. Ultimately, we will determine if corresponding nonlinear models are justified. We also plan to use Memphis data and meet with end users.

REFERENCES

Box, G. E. P. and G. M. Jenkins, 1976: *Time Series Analysis, Forecasting, and Control (2nd ed.)*, Holden-Day, San Francisco.

Cole, R. E., F. W. Wilson, J. A. McGinley, and S. C. Albers, 1993: ITWS gridded analyses. Preprints, *Fifth International Conference on Aviation Weather Systems*, Vienna, Virginia, American Meteorological Society.

Delanoy, R. L. and S. W. Troxel, 1993: A machine intelligent gust from algorithm for Doppler radars. Preprints, *Fifth International Conference on Aviation Weather Systems*, Vienna, Virginia, American Meteorological Society.

Gelb, A. (ed.), 1974: *Applied Optimal Estimation*, MIT Press, Cambridge, MA.

Gershenfeld, N. A. and A. S. Weigend, 1993: The future of time series, learning and understanding. *Proceedings Volume XV, Santa Fe Institute Studies in the Sciences of Complexity*, Addison-Wesley, Reading, MA.

Harvey, A. C., 1989: *Forecasting, Structural Time Series Models and the Kalman Filter*, Cambridge University Press, Cambridge.